

Supplementary Information

Supplementary Figures

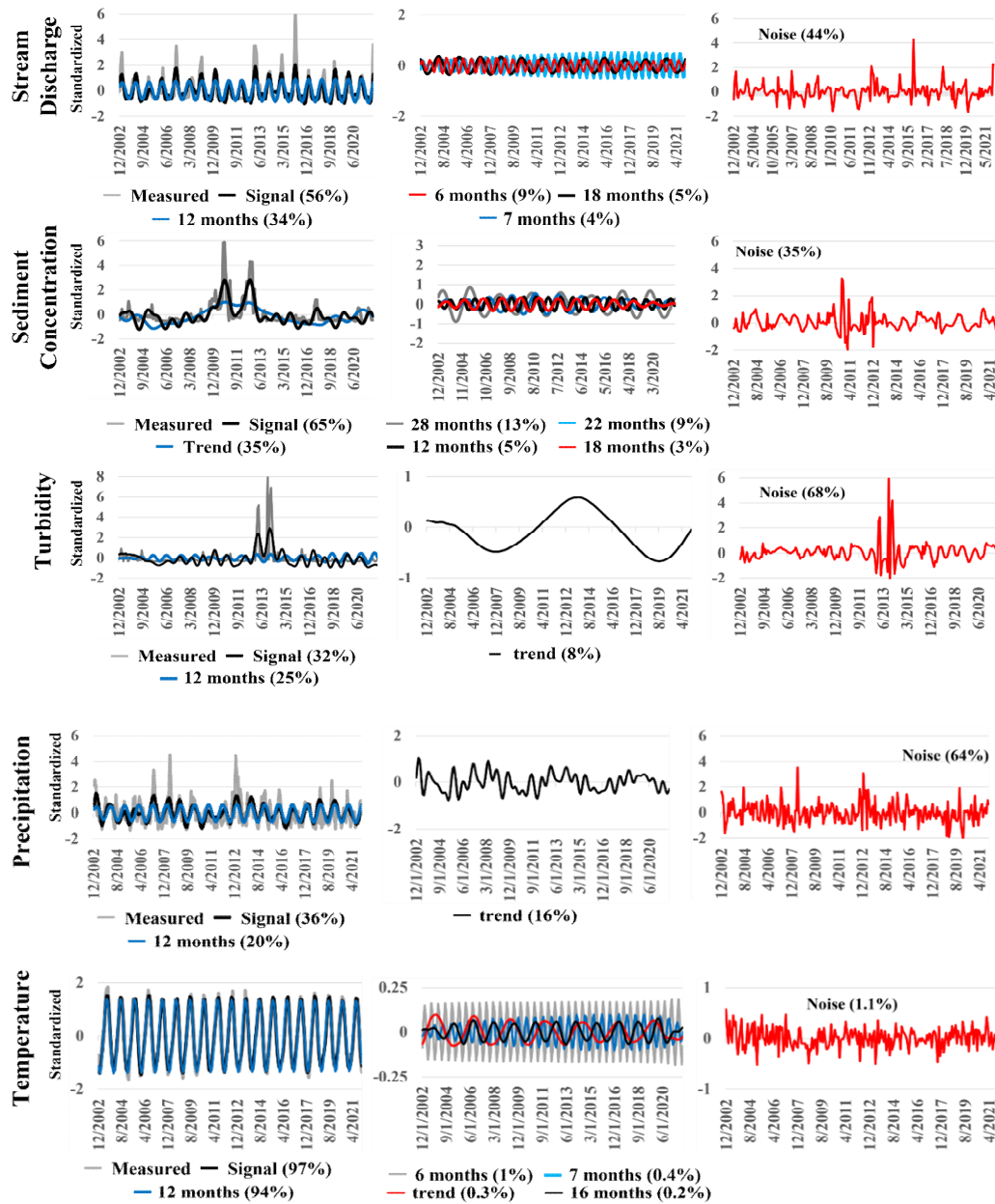


Figure S1. Signal processing of observed watershed covariates. For each covariate, the leftward graph plots the observed record (grey curve), isolated signal (black curve), and dominant annual cycle or low-term nonlinear trend cycle (blue curve). The middle graph plots other oscillatory components. The rightward graph plots unstructured noise. The percentages in parentheses measure signal strengths of signal and noise components. This signal processing information is summarized in Table 1.

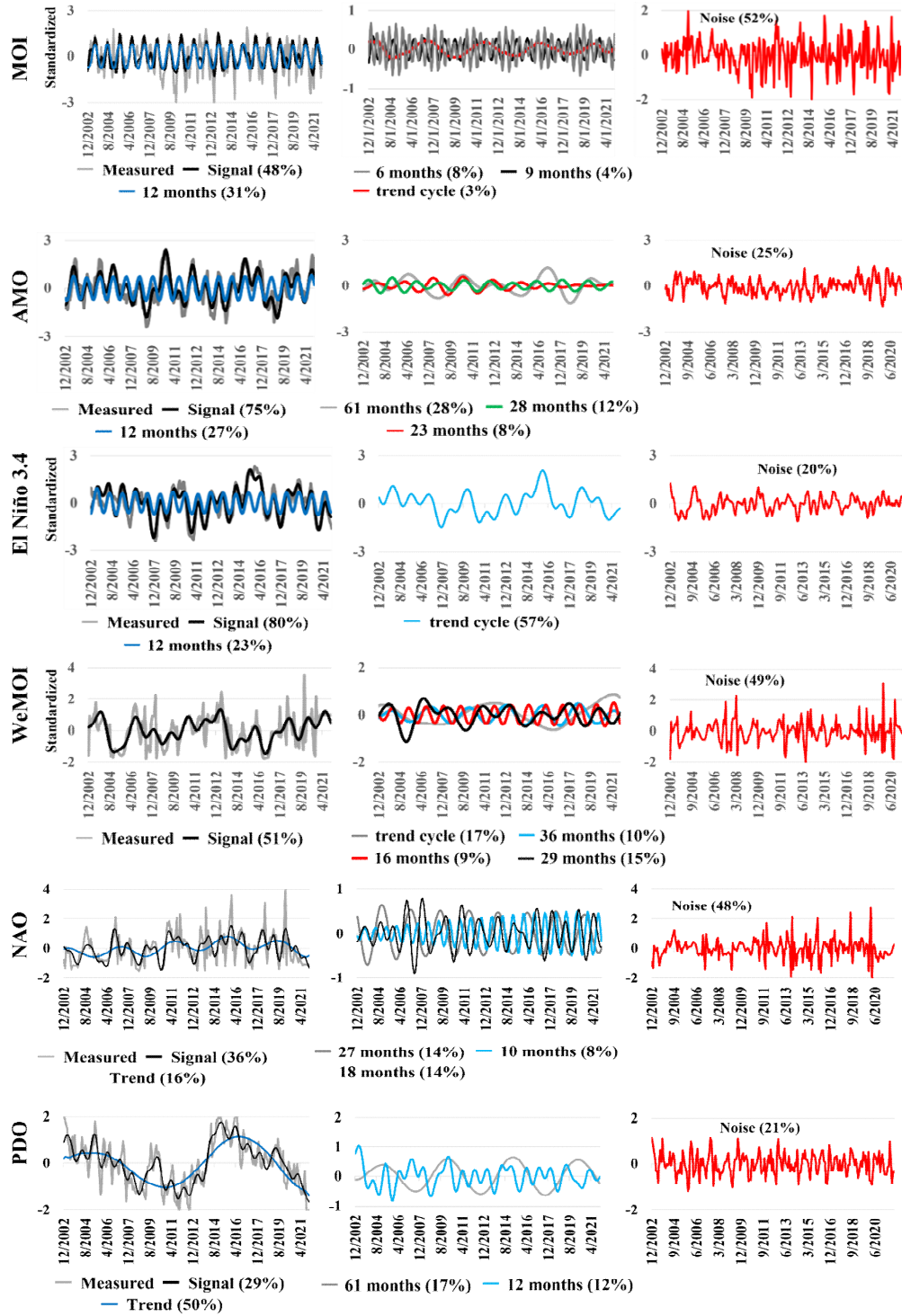


Figure S2. Signal processing of climatic teleconnections. See legend to Fig. S1.

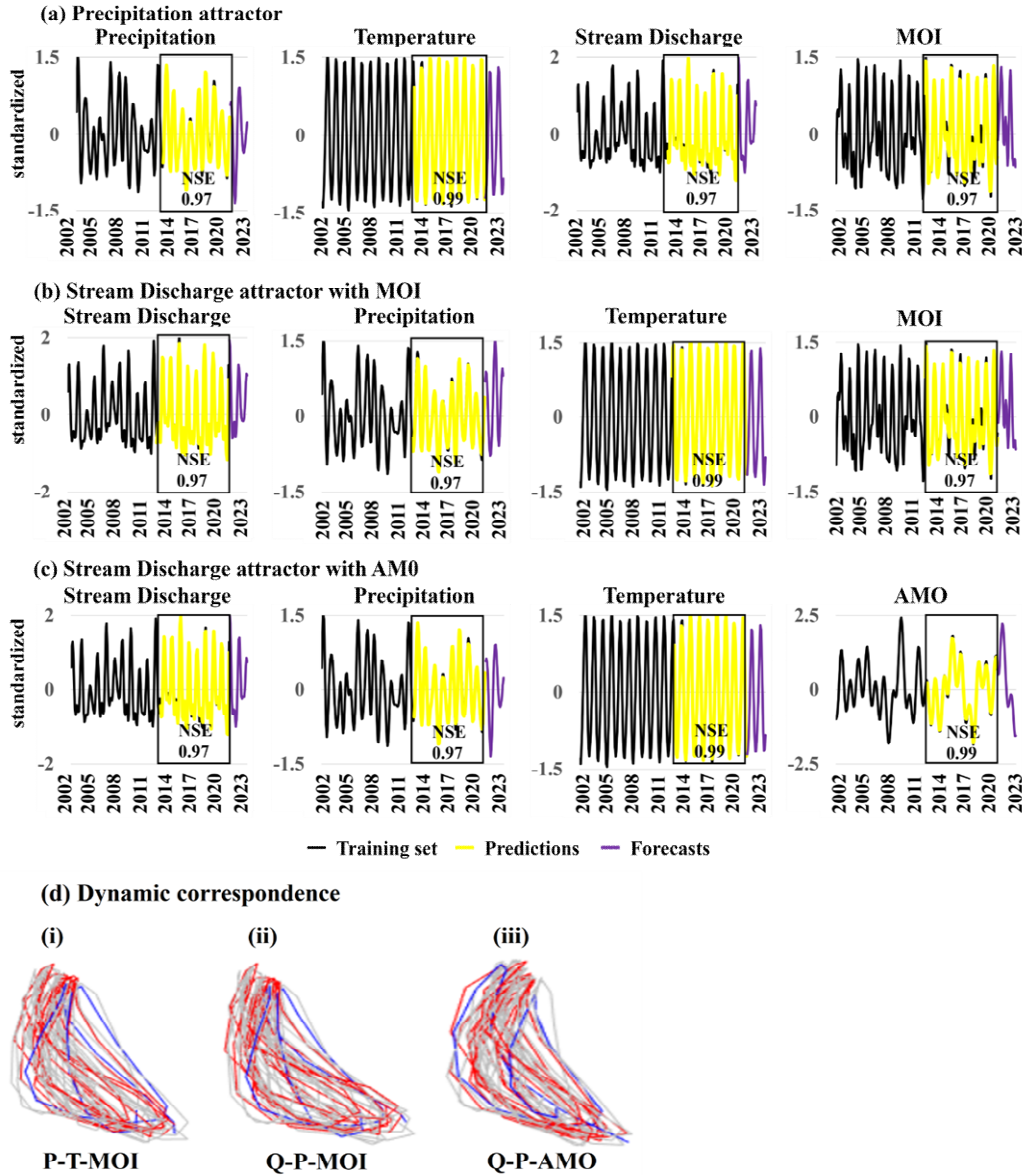
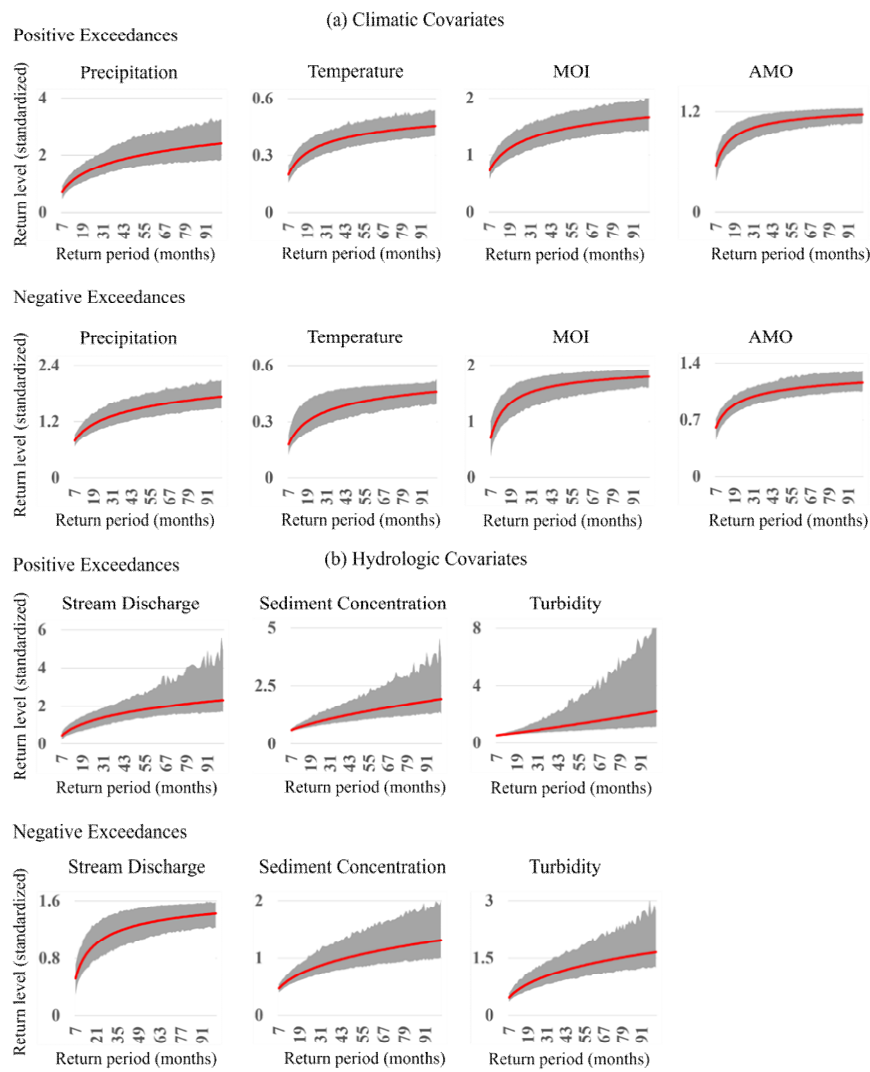


Figure S3. Performance of echo-state neural networks in reproducing resilience attractors. The figure shows performance plots for reproductions of resilience attractors (constructed in Fig. 6) made with echo state neural networks (ESNN). The plot for each signal component of a reproduced attractor (Figs. S3(a)-(c)), shows the portion of the signal allocated to the training set (black curve to left of box), the portion remaining in the testing set (boxed area), ESNN in-sample predictions (yellow curve in box), and two-year ESNN out-of-sample forecasts (violate curve to right of box). ESNN predicted each signal with almost-perfect skill ($NSE > 0.97$). Forecasts largely preserved oscillatory behavior observed in corresponding signals. In a demonstration of dynamic correspondence, state-space trajectories reconstructed from ESNN in-sample predictions (blue line) and out-of-sample forecasts (red line) largely rested on attractors constructed from in-sample signals (black line) (Fig. S3(d)).



(c) Summary Table

Covariate	Positive Noise				Negative Noise			
	Threshold	1 year	2 years	3 years	Threshold	1 year	2 years	3 years
Precipitation	0.69	1.06	1.49	1.75	0.78	0.99	1.23	1.39
Temperature	0.19	0.26	0.34	0.37	0.17	0.25	0.33	0.37
MOI	0.71	0.95	1.20	1.34	0.66	1.09	1.43	1.57
AMO	0.52	0.77	0.95	1.03	0.58	0.77	0.94	1.01
Stream Discharge	0.41	0.77	1.22	1.51	0.47	0.79	1.06	1.18
Sediment Concentration	0.59	0.73	0.97	1.17	0.45	0.59	0.79	0.92
Turbidity	0.53	0.61	0.80	1.01	0.45	0.64	0.91	1.10

Figure S4. Extreme Value Analysis of climatic and watershed covariates. This figure displays return-level plots of extreme (standardized) noise isolated from (a) climate covariates and (b) watershed covariates with extreme value statistics. Positive (negative) exceedances occur when observed values are greater (less) than corresponding signal values. We defined positive noise extremes as those exceeding the upper 15th percentile threshold, and the absolute value of negative noise extremes in the same manner. Return-levels in each plot increase at a decreasing rate with return time as generally expected. In Fig. S4(c), positive and negative noise extremes expected over 1-year, 2-year, and 3-year return times are summarized.

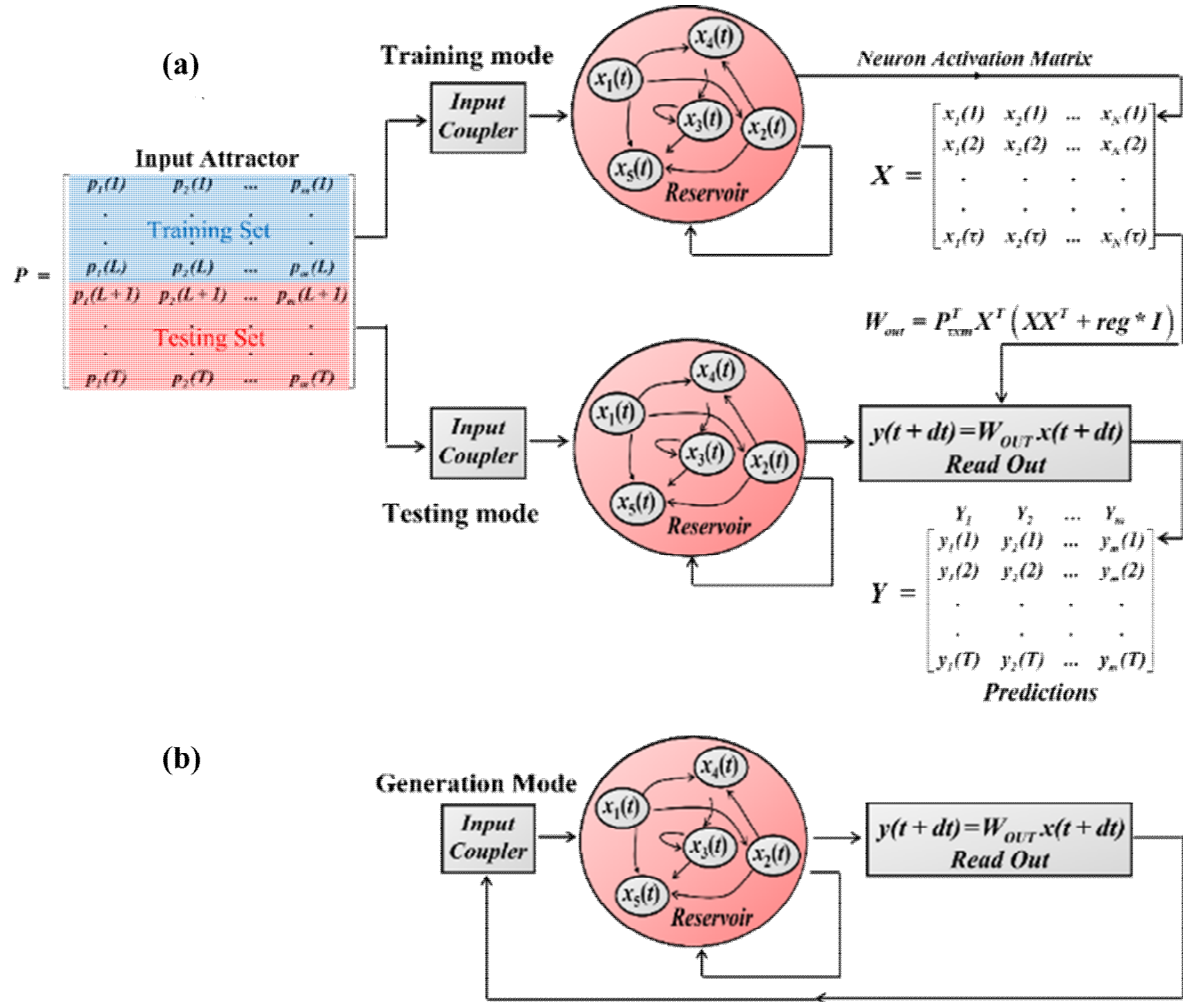


Figure S5. ESNN operation: (a) Training mode; (b) Generation mode.

Supplementary Tables

Hyperparameters	Description	Attractors	
		Q-P-T-MOI ^a	Q-P-T-AMO
tau	Fraction of attractor points in learning set	0.55	0.56
N	Number of neural states in reservoir	2746	3003
rho-scale	Spectral radius of reservoir	1.07	0.68
leaking_rate	Updating of neural states	0.88	0.91
reg	Tikhonov regularization coefficient	$10^{-5.65}$	$10^{-5.81}$
a	Interval of uniform random values used to construct input coupler	(0.68, 2)	(0.65, 2)
b	Interval of uniform random values used to construct reservoir	(0.35, 2)	(0.87, 2)

^a Variables: Q (stream discharge), P (precipitation), T (temperature), MOI (Mediterranean Oscillation Index), AMO (Atlantic Multidecadal Oscillation).

Table S1. ESNN hyperparameter values used to reproduce attractors reconstructed from watershed records.